(mirror plane), S_2 (inversion center), or S_4 axes.
25. J. T. Groves and R. S. Meyers, *J. Am. Chem. Soc.* **105**, 5791 (1983).
26. S. O'Malley and T. Kodadek, *ibid.* **111**, 9116 (1989).
27. Note that a chiral porphyrin may be formed by bridging a prochiral macrocycle with an achiral strap (*20*) or by attaching a porphyrin to a prochiral bridge.
28. D. Mansuy, P. Battioni, J.-P. Renaud, P. Guerin, *J. Chem. Soc. Chem. Commun.* **1985**, 155 (1985).
29. S. Licoccia *et al.*, *Magn. Reson. Chem.* **29**, 1084 (1991).
30. P. Maillard, J. L. Guerquin-Kern, M. Momenteau, *Tetrahedron Lett.* **32**, 4904 (1991).
31. R. L. Halterman and S.-T. Jan, *J. Org. Chem.* **56**, 5253 (1991).
32. J. P. Collman, X. Zhang, V. J. Lee, J. I. Brauman, *J. Chem. Soc. Chem. Commun.* **1992**, 1647 (1992).
33. J. T. Groves and P. Viski, *J. Org. Chem.* **55**, 3628 (1990).
34. J. P. Collman *et al.*, *J. Am. Chem. Soc.* **110**, 3477 (1988).
35. Y. Naruta, F. Tani, K. Maruyama, *Chem. Lett.* **1989**, 1269 (1989); Y. Naruta, F. Tani, N. Ishihara, K. Maruyama, *J. Am. Chem. Soc.* **113**, 6865 (1991); Y. Naruta, N. Ishihara, F. Tani, K. Maruyama, *Bull. Chem. Soc. Jpn.* **66**, 158 (1993).
36. J. P. Collman, V. J. Lee, X. Zhang, J. A. Ibers, J. I. Brauman, *J. Am. Chem. Soc.* **115**, 3834 (1993); J. P. Collman *et al.*, in preparation.
37. E. G. Samsel, K. Srinivasan, J. K. Kochi, *J. Am. Chem. Soc.* **107**, 7606 (1985); K. Srinivasan, P. Michaud, J. K. Kochi, *ibid.* **108**, 2309 (1986).
38. W. Zhang, J. L. Loebach, S. R. Wilson, E. N. Jacobsen, *ibid.* **112**, 2801 (1990).
39. W. Zhang and E. N. Jacobsen, *J. Org. Chem.* **56**, 2296 (1991); E. N. Jacobsen, W. Zhang, M. Güler, *J. Am. Chem. Soc.* **113**, 6703 (1991); E. N. Jacobsen, W. Zhang, A. R. Muci, J. R. Ecker, L. Ding, *ibid.*, p. 7063; N. H. Lee and E. N. Jacobsen, *Tetrahedron Lett.* **32**, 6533 (1991); N. H. Lee, A. R. Muci, E. N. Jacobsen, *ibid.*, p. 5055; E. N. Jacobsen and L. Deng, *J. Org. Chem.* **57**, 4320 (1992).
40. R. Irie, K. Noda, Y. Ito, N. Matsumoto, T. Katsuki, *Tetrahedron Lett.* **31**, 7345 (1990); *Tetrahedron Asymmetry* **2**, 481 (1990); R. Irie, K. Noda, Y. Ito, T. Katsuki, *Tetrahedron Lett.* **32**, 1055 (1991).
41. T. Yamada, K. Imagawa, T. Nagata, T. Mukaiyama, *Chem. Lett.* **1992**, 2231 (1992); T. Mukaiyama, T. Yamada, T. Nagata, K. Imagawa, *ibid.* **1993**, 327 (1993).
42. Low turnover numbers continue to inhibit the development of practical enantioselective epoxidation catalysts derived from metalloporphyrins or metallosalens. Oxidative decomposition of the porphyrin and oxidative decomposition of the porphyrin superstructure have fundamentally different consequences and can depend on the choice of oxidant and solvent used to generate the active metal-oxo species. Porphyrin oxidation, diagnosed by changes in the ultraviolet-visible spectrum, deactivates the catalyst. However, oxidation of the porphyrin superstructure typically does not perturb this spectrum but may increase the rate of catalysis and seriously diminish the selectivity by opening up the steric environment. It is therefore critical to follow the spectroscopy and product distribution of the reactions as a function of time and catalyst turnover. Mass spectroscopy may be useful for characterizing metalloporphyrin catalysts that have had their superstructures only partially decomposed. For metallosalens, the facile oxidizability of the imine is an inherent problem that conceptually resembles the vulnerability of unsubstituted porphyrins to oxidation at the *meso* position. Metallosalen decomposition may be followed by ultraviolet-visible spectroscopy; fortunately, the decomposition products are catalytically incompetent and selectivity is not compromised.
43. We thank NIH for financial support (grant 5R37-GM 17880). X.Z. thanks the Stanford Chemistry Department for a Franklin Veatch Fellowship, and E.S.U. thanks NIH for a postdoctoral fellowship.

RESEARCH ARTICLES

Isolation of New Ribozymes from a Large Pool of Random Sequences

David P. Bartel and Jack W. Szostak

An iterative in vitro selection procedure was used to isolate a new class of catalytic RNAs (ribozymes) from a large pool of random-sequence RNA molecules. These ribozymes ligate two RNA molecules that are aligned on a template by catalyzing the attack of a 3′-hydroxyl on an adjacent 5′-triphosphate—a reaction similar to that employed by the familiar protein enzymes that synthesize RNA. The corresponding uncatalyzed reaction also yields a 3′,5′-phosphodiester bond. In vitro evolution of the population of new ribozymes led to improvement of the average ligation activity and the emergence of ribozymes with reaction rates 7 million times faster than the uncatalyzed reaction rate.

A current view of early evolution is that modern-day life descended from an "RNA world," an era (before proteins) in which all macromolecular catalysts were ribozymes (*1*). One of the most important enzymes of the RNA world would have been an RNA replicase, an RNA molecule capable of autocatalytic replication by virtue of its ability to fulfill two seemingly opposed functions at different times—either folding into an RNA polymerase that uses RNA as a template, or unfolding and acting as a template for another replicase molecule. Previous efforts to design RNA molecules with polymerase and replicase activities have focused on modifying known ribozymes derived from the group I self-splicing introns (*2, 3*). Although progress has been made on this front, the development of iterative in vitro selection techniques has led to the possibility of isolating such enzymes from completely random-sequence RNA, without bias toward any known sequence or structure. This prospect is appealing in that some versions of the RNA world hypothesis suggest that the first enzyme in the origin of life was a replicase that arose from a prebiotic pool of random RNA or RNA-like sequences (*1*).

Repeated cycles of in vitro selection and in vitro amplification have been widely used to isolate, from large pools of random or degenerate sequences, rare nucleic acid sequences with specified biochemical properties (*4*). Such methods have been used to define protein binding sites on DNA and RNA molecules, to isolate RNAs and DNAs with specific binding sites for a variety of small molecule ligands, and to select for modified catalytic activities from existing ribozymes. We now show that in vitro selection and evolution techniques can be used to generate new classes of ribozymes that catalyze a reaction analogous to a single nucleotide addition during RNA polymerization.

Our selection protocol was designed to effect the enrichment of catalytically active members of a pool of RNA molecules on the basis of their ability to ligate a substrate oligonucleotide to their own 5′ end. The substrate sequence was then used as a tag to separate the rare ligated members of the pool from inactive molecules. We used a substrate oligonucleotide designed to anneal with part of a template region within the 5′ constant region of the pool RNA (Fig. 1A). The pool RNA began with a triphosphate, positioned next to the 3′-hydroxyl of the substrate oligonucleotide by base-pairing of the first few nucleotides of the pool RNA to the remainder of the template region, thus forming an interrupted stem loop. Ligation of the substrate oligonucleotide to the pool RNA was designed to be analogous to chain elongation by one nucleotide during RNA polymerization: in both cases, the growing strand and the triphos-

The authors are with the Department of Molecular Biology, Massachusetts General Hospital, Boston, MA 02114.

phate-containing substrate base pair to a template, the 3′-hydroxyl of the growing strand attacks the α-phosphate of a 5′-triphosphate, and pyrophosphate is displaced with the concomitant formation of a 3′,5′-phosphodiester bond (Fig. 1). In its overall substrate configuration, the reaction resembles group I intron self-splicing because the substrates and the template are covalently linked to the catalytic sequences.

Pool construction and design. We sought to maximize the number and length of the sequences in the initial random-sequence pool in order to maximize the likelihood of finding a sequence with catalytic activity. A large random region provides not only a linear advantage in finding a given sequence element but, more significantly, a combinatorial advantage in finding sets of sequence segments that interact to form a given RNA structure (5). However, the chemical synthesis of very long oligonucleotides is difficult, and both the yield and quality of the DNA decline substantially with increasing length (6).

This problem was avoided by linking smaller DNA pools to generate one larger pool that had 1.6×10^{15} different molecules, each with a central region containing 220 random positions (Fig. 2). This pool was amplified by the polymerase chain reaction (PCR) and then transcribed in vitro to yield a pool of RNA sequences (pool 0 RNA). The use of a such a large random region precludes the possibility of sampling more than a minute fraction of all possible (4^{220}) sequences. Thus, for a selection based on catalysis to succeed, the catalytically active RNAs must have structures that are simple enough to be constructed from relatively common sequences. Alternatively, if a complex structure is required, there must be very many such distinct structures in order for one to be present by chance in the random-sequence pool.

Selection for catalytic RNAs. Because sequence space can only be sparsely sampled, any catalyst present in the pool would probably only be a suboptimal example of its respective structural class. We therefore used incubation conditions during the initial ligation reactions that were known to stabilize marginal RNA structures and restore the activity of suboptimal ribozyme variants. However, incubation of the pool RNA under such conditions led to rapid and extensive aggregation; more than half of the pool RNA precipitated when incubated for 90 minutes at 37°C in high concentrations of Mg^{2+} and monovalent ions (50 mM $MgCl_2$, 500 mM KCl, 0.5 μM RNA), and precipitation was even more rapid at higher temperatures. It appears that conditions that favor RNA intramolecular structure also stabilize intermolecular interactions; as molecules find regions of complementarity with more than one other molecule, RNA networks form and eventually become too large to remain in solution (7).

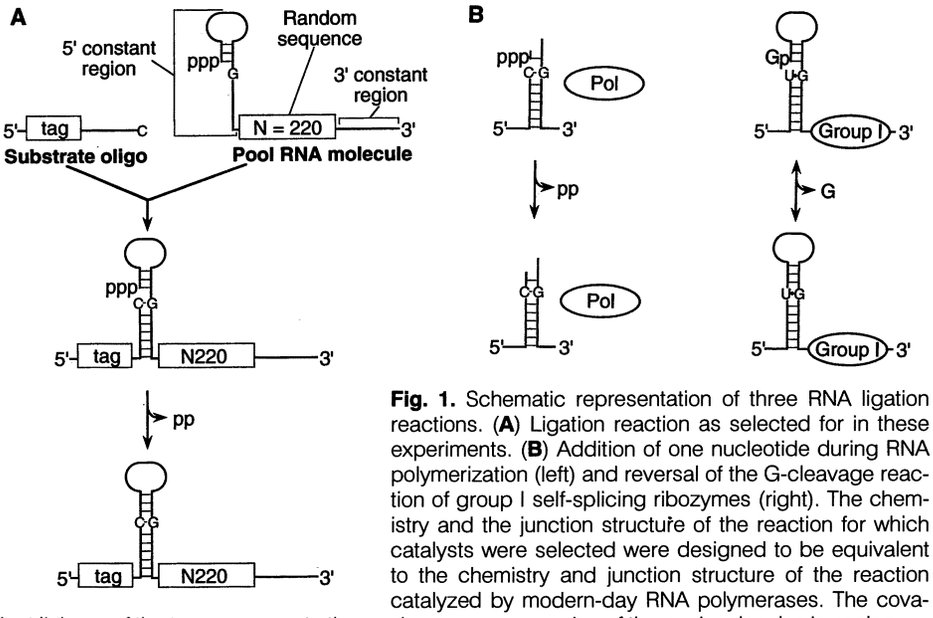

Fig. 1. Schematic representation of three RNA ligation reactions. (**A**) Ligation reaction as selected for in these experiments. (**B**) Addition of one nucleotide during RNA polymerization (left) and reversal of the G-cleavage reaction of group I self-splicing ribozymes (right). The chemistry and the junction structure of the reaction for which catalysts were selected were designed to be equivalent to the chemistry and junction structure of the reaction catalyzed by modern-day RNA polymerases. The covalent linkage of the tag sequence to the random-sequence region of the pool molecules is analogous to the linkage of the 5′ exon to a group I intron.

To minimize the problem of RNA aggregation, we immobilized the pool of RNA molecules on agarose beads before the addition of Mg^{2+} (Fig. 3). A biotinylated oligonucleotide was annealed to the 3′ constant region of the pool RNA, and the mixture was then incubated with avidin-agarose beads. Once tethered to the agarose, the pool molecules could not diffuse and form intermolecular interactions, and could therefore be safely incubated with the substrate oligonucleotide overnight in the presence of a high concentration of Mg^{2+}. During this incubation, the temperature was cycled between 25° and 37°C to encourage individual RNA molecules to explore alternate conformations, so that fewer potentially active molecules would be locked in unproductive metastable conformations. After this ligation incubation, the pool RNA was eluted from the agarose and subjected to a two-step procedure to enrich for sequences that had successfully ligated the substrate to their 5′ terminus (Fig. 3) (3). First, an oligonucleotide affinity column was used to selectively bind molecules containing the "tag" sequence of the substrate oligonucleotide. RNAs that bound to this column were eluted and reverse tran-

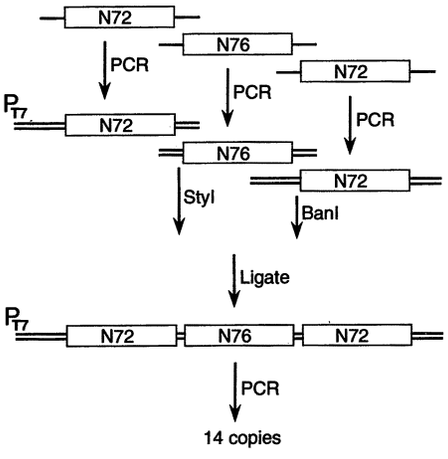

Fig. 2. Pool construction. The DNA template for the initial RNA pool (pool 0 RNA) was constructed by joining DNA fragments derived from two shorter pools, pools N72 and N76 (*28*). The N72 and N76 pools were digested with the indicated enzymes that trim off much of the defined sequence and leave non-palindromic 5′ extensions suitable for the directional ligation of N72 fragments to both ends of the N76 fragment. The ligation reaction yielded 540 μg of full-length DNA, which corresponds to 1.6×10^{15} different 294-bp molecules. This ligated product (pool 0 DNA) has a central 232-bp segment that contains 220 random positions punctuated by two 6-bp restriction sites. The central segment is flanked by two constant segments; at one end a 42-bp segment contains the T7 promotor (P_{T7}) and also codes for the 5′ constant region that binds the substrate oligonucleotide and participates in the ligation reaction (Fig. 1), and at the other end a 20-bp segment codes for the 3′ constant region (*29*). Large-scale PCR (400 ml, four cycles) was used to generate multiple copies of pool 0 DNA so that the pool can also be used for other selection experiments. Two equivalents of pool 0 DNA (2×540 μg; 1.4×10^{15} different sequences represented at least once) were transcribed in vitro to generate the initial RNA pool (pool 0 RNA).

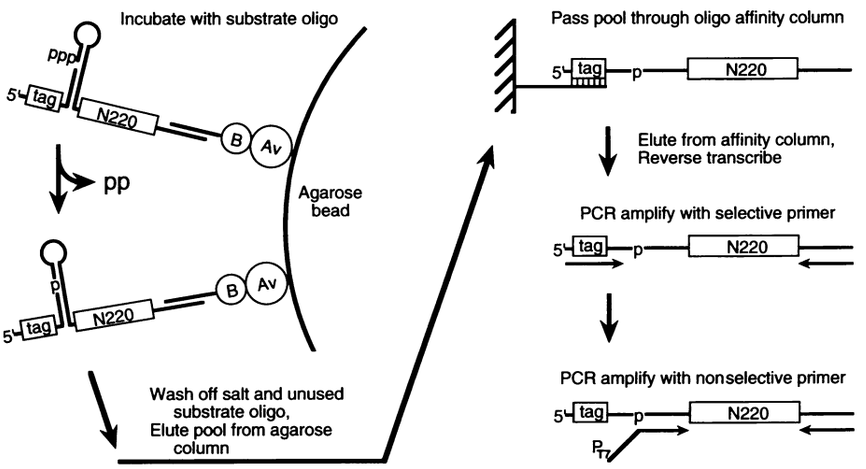

Fig. 3. Ligation and selection scheme for rounds 1 to 4. RNA was immobilized on streptavidin-agarose beads by means of a biotinylated DNA oligonucleotide designed to anneal to the 3′ constant region of the pool RNA (*30*). The unbound pool RNA was washed away, and the beads were equilibrated with ligation buffer without $MgCl_2$ (30 mM tris, pH 7.4, 600 mM KCl, 1 mM EDTA, 0.1 percent NP-40). After 10 minutes at room temperature, $MgCl_2$ was added (final concentration, 60 mM). The substrate oligonucleotide (2.5 to 6 μM) was then incubated with the immobilized pool for 16 hours, with temperature cycling between 25° and 37°C, such that the reaction was at 25°C for 75 percent of the time. Salts and unreacted substrate were then washed from the beads, and the pool was eluted with mild alkali (10 mM NaOH, 1 mM EDTA) to disrupt hybridization of the pool RNA to the biotinylated oligonucleotide. The pool RNA was collected, neutralized, concentrated, and the amount of RNA indicated in Table 1 was then passed through an oligonucleotide affinity column complementary to the substrate tag sequence. Different pairs of affinity columns and substrate tags (*31*) (Table 1) were used in each of the first four rounds to minimize enrichment of inactive molecules with chance affinity to a given column. Molecules captured on the affinity column were eluted, reverse-transcribed, and PCR-amplified for 10 cycles with a selective primer with the substrate tag sequence and a second primer complementary to the 3′ constant region. Finally, a nonselective PCR reaction regenerated molecules of the same structure as the pool 0 DNA (*32*). Rounds 5 to 10 used the same general selection strategy as the first four rounds, with some modifications in the ligation conditions (Table 1) to increase the stringency of the ligation reaction. Pool RNA was not immobilized on agarose during reactions for rounds 6 to 10 (*33*).

scribed. In the second selection step, a PCR primer complementary to the tag region of the cDNA was used to selectively amplify cDNAs derived from ligated RNA sequences. RNA with the original unligated structure was then regenerated by nested PCR and in vitro transcription. This RNA pool (pool 1 RNA) was further enriched in active sequences by a second round of ligation, selection, and amplification (yielding pool 2 RNA); the process was repeated for a total of 10 rounds of ligation, selection, and amplification (Table 1).

Catalyzed and noncatalyzed ligation. Successful enrichment of active sequences was readily apparent after four rounds of selection (Fig. 4A). Nearly 3 percent of pool 4 RNA became ligated to the substrate oligonucleotide during the first hour of incubation. The time course of the ligation reaction with RNA from pool 4, and with RNA from all other selected pools, was nonlinear. The faster rate at the earliest time points is probably due to the heterogeneous nature of the pool RNA, which consisted of a mixture of sequences with differing activities, and which may also have contained a significant proportion of molecules trapped in inactive conformations (*8*). Throughout the work described in this article we have calculated pool ligation rates based on the earliest time point that can be accurately measured, typically the time point in which 2 percent of the pool RNA has become ligated. Rates calculated from early time points are a reflection of the average ligation rate of the population of molecules, but they may be greater than the median activity, because ligated molecules of early time points involve a disproportionate number of the most active sequences.

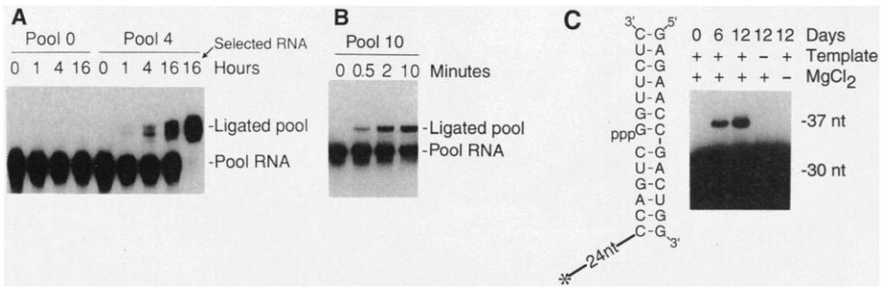

Fig. 4. (**A**) Time course of the catalyzed reaction. Phosphorus-32–labeled RNA of pools 0 and 4 was immobilized on agarose beads and incubated with substrate oligonucleotide. At the indicated time samples of the reaction were removed and stopped by addition of EDTA. RNA was eluted from the beads and separated by electrophoresis on a 4 percent acrylamide–7 M urea gel. A portion of the 16-hour pool 4 reaction was enriched for ligated molecules on an oligonucleotide affinity column ("selected RNA"). Immobilization, ligation, elution, and affinity selection conditions were as described for the first rounds of selection (Fig. 3). PhosphorImager (Molecular Dynamics) or Betagen (IntelliGenetics) scans were used for ^{32}P quantitation throughout. (**B**) Time course of pool 10 RNA ligation. Uniformly labeled pool RNA (0.4 μM) was annealed (*33*), and then incubated at 25°C with substrate oligonucleotide (2.5 μM) in the ligation buffer of the initial rounds (Fig. 3). Samples of the reaction were stopped with EDTA, and the RNA was separated on a 6 percent acrylamide–7 M urea gel. (**C**) Time course of the uncatalyzed reaction and template and magnesium dependence of this reaction. The 30-nt molecule that had been used as a substrate oligonucleotide in the catalyzed reaction was ^{32}P end-labeled (indicated by an asterisk), and this labeled oligonucleotide (0.4 μM) was incubated together with a 13-nt template RNA (20 μM) and a 7-nt RNA that has a 5′ terminal triphosphate (20 μM). Buffer and temperature conditions were as in Fig. 3. Where indicated, the template RNA was omitted, or the $MgCl_2$ was replaced by 5 mM EDTA.

Having detected both the catalyzed and uncatalyzed ligation reactions, we confirmed the formation of the expected reaction products. Sequence analysis of ligated pool 4 RNA (Fig. 5A) indicated that no

nucleotides were lost during the catalyzed ligation reaction, ruling out the possibility of contamination by a group I ribozyme-like activity (which would displace the 5′-guanosine of the pool RNA). Inorganic pyrophosphate was identified as a product of the catalyzed reaction by thin-layer chromatography (Fig. 5B). The regiospecificity of the reaction, that is, the formation of 3′,5′- as opposed to 2′,5′-phosphodiester bonds, was determined by purifying ligated RNA from both the catalyzed and the uncatalyzed reactions, and examining the products of digestion with a nuclease of known specificity (Fig. 5C). No 2′-linked digestion products could be detected (limits of detection 0.5 percent), showing that both reactions yielded at least 200 times more 3′-linked product than 2′-linked product. This analysis also confirmed the ligation junction sequence of the uncatalyzed reaction.

In vitro evolution. In vitro selection and directed in vitro evolution have been used to select for variants of group I ribozymes with enhanced or altered activities (*3*, *10*), and to select for RNAs that self-cleave in the presence of Pb^{2+}, starting from a partially randomized tRNA that binds and self-cleaves in the presence of Pb^{2+} (*11*). We used similar methods to enhance the activity of the selected pool of ribozymes by introducing random mutations into the pool 4 DNA and selecting for more active variants. To generate a broad spectrum of pool 4 variants, four samples of pool 4 DNA were subjected to error-prone PCR for 0, 30, 60, and 90 doublings, corresponding to expected mutation rates of about 0, 2, 4, and 6 percent per residue, respectively (*12*). Equal amounts of RNA transcribed from each of the subpools were mixed and subjected to another cycle of ligation, selection, and amplification (round 5). The duration of the round 5 ligation step was reduced to 30 minutes because such a large portion of the pool 4 RNA ligates in 16 hours. Rounds 6 and 7 also included PCR mutagenesis and progressively shorter ligation incubations (Table 1).

All of the elements of directed in vitro evolution (*10*) were in place during rounds

Table 1. Selection summary. General ligation and selection procedures were as described in Fig. 3.

Round	Error-prone PCR*	Ligation conditions†		Fraction ligated	Affinity selection		Ligation rate after selection (per hour)‡
		$MgCl_2$ (mM)	Time (hour)		RNA (μg)	Column	
0							0.000003
1	No	60	16	0.00005	1600§	dT cellulose	<0.000004
2	No	60	16	<0.00007	27	dA cellulose	0.0008
3	No	60	16	0.014	15	dT magnetic	0.0094
4	No	60	16	0.16	6	dGAGAT . . . Teflon	0.027
5	Yes	60	0.50	0.013	30	dGAGAT . . . Teflon	0.16
6	Yes	60	0.17	0.026	29	dGAGAT . . . Teflon	0.40
7	Yes	60	0.02	0.007	10	dGAGAT . . . Teflon	0.86
8	No	4	0.12	0.005	32	dGAGAT . . . Teflon	3.2
9	No	2.5	0.17	0.003	37	dGAGAT . . . Teflon	4.5
10	No	2.5	0.17	0.005	8	dT magnetic	8.0

*Template DNA mutagenized (*12*) prior to transcription. †In rounds 1 to 5, the ligation was performed with the pool immobilized on an agarose column; in rounds 6 to 10 the ligation was done in solution. ‡Ligation rate assays are described in Fig. 7. §More than six pool equivalents of RNA.

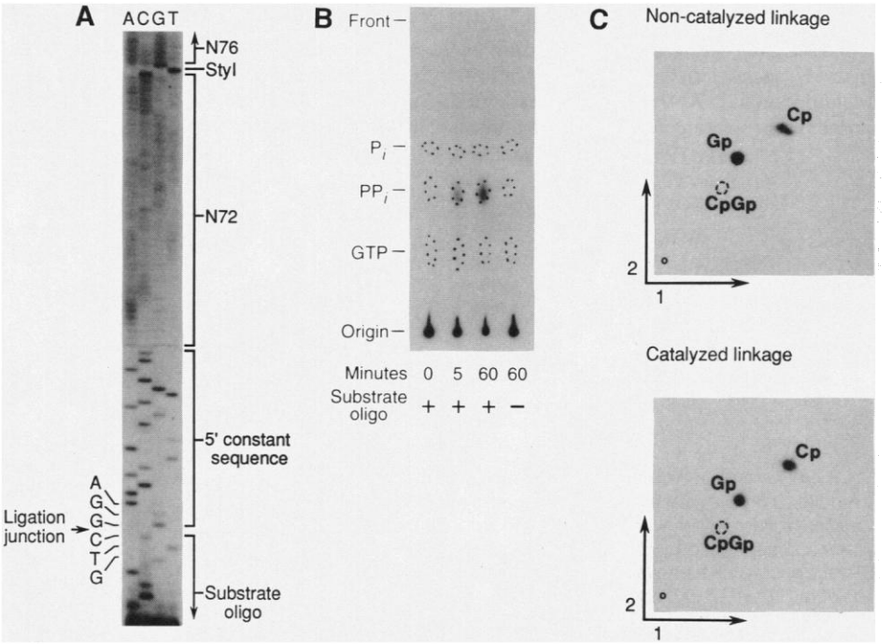

Fig. 5. Characterization of catalyzed and uncatalyzed ligation. (**A**) The expected ligation junction sequence revealed by batch sequencing. Pool DNA from the round 5 selective amplification was gel-purified and PCR-sequenced (Boehringer Mannheim) with ^{32}P end-labeled selective primer. (**B**) Inorganic pyrophosphate release during ligation. Pool 10 RNA (1 μM) that had been labeled by transcription in the presence of [γ-^{32}P]GTP (guanosine triphosphate) was annealed (*33*) and then incubated in tris (30 mM, pH 7.4), KCl (200 mM), $MgCl_2$ (15 mM), and EDTA (150 μM) with or without substrate oligonucleotide (2.5 μM). At the indicated time, the reaction was stopped with EDTA and co-spotted onto PEI-cellulose thin-layer chromatography (TLC) plates with KH_2PO_4 (P_i), $Na_3HP_2O_7$ (PP_i), and GTP (5 nmol each). The TLC was performed in 0.5 M HCl. The positions of the unlabeled markers (dashed lines) were visualized (*34*) and compared to the autoradiograph to identify the leaving group of the ligation reaction. (**C**) Complete ribonuclease T2 digestion of ligation products to nucleoside monophosphates indicating that both catalyzed and uncatalyzed reactions form predominantly 3′,5′ linkages. The uncatalyzed ligation was as in Fig. 4C, except template (16 μM) and unlabeled 30-nt (21 μM) oligonucleotides were incubated with the 7-nt RNA (15 μM) that had been labeled by transcription with [α-^{32}P]GTP (pp*G*GpUpUpCpUpC, where the asterisk indicates a labeled phosphate). The catalyzed reaction was done with the same unlabeled 30-nt and labeled 7-nt oligonucleotides (2 μM each), but the 13-nt template RNA was replaced by pool 6 RNA catalytic sequences (2 μM) that had modified 5′ constant regions designed to hybridize to the substrate oligonucleotides (5′ constant region: GAGAACCGACUGGCACC). After incubation for 23 days (uncatalyzed) or overnight (catalyzed), the 37-nt products (5′-24-nt-CCAGUC*G*GUUCAC) were gel-purified. The isolated products (less than 5 ng) were digested with ribonuclease T2 (BRL) in the presence of a 13-nt carrier RNA (10 μg) analogous to a 2′-linked ligation junction (5′-CCAGUC^GGUUCAC; the symbol ^ indicates 2′,5′ linkage, synthesized with ChemGene phosphoramidites). Digestion products were separated by TLC in two dimensions (*35*) on PEI-cellulose plates (9 by 9 cm) with a fluorescent indicator (Baker). Ultraviolet shadowing revealed the carrier RNA digestion products, including the 2′-linked GpCp dinucleotide (dashed circle) as well as the C and G nucleoside 3′-monophosphates. The small solid circle indicates the origin.

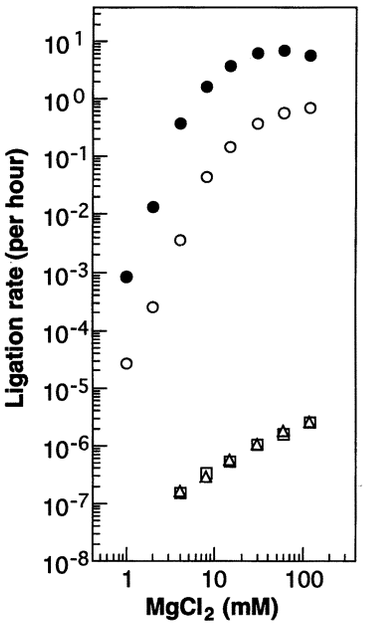

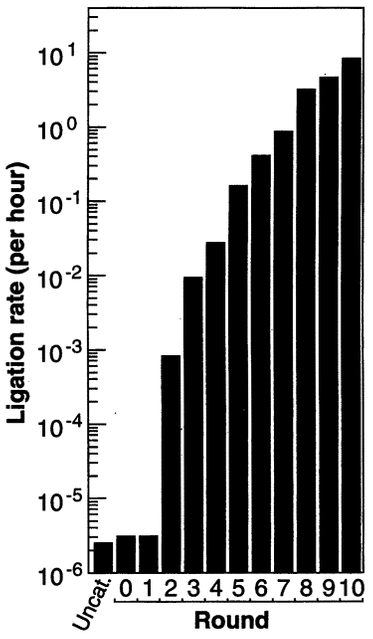

Fig. 6 (left). Mg^{2+} dependence of pool 10, pool 7, and uncatalyzed ligation. Pool 7 (open circles) and pool 10 (closed circles) RNA ligation time courses were performed in tris (30 mM, pH 7.4), KCl (200 mM), NaCl (2.5 mM), $MgCl_2$ (1 to 120 mM), and EDTA (1 percent of Mg^{2+} concentration) at 25°C as described in Fig. 4B. The uncatalyzed reaction was assayed in the same ligation buffers by incubating (12 days, 25°C) end-labeled substrate oligonucleotide (0.4 μM) with a 22-nt RNA identical to the 5′ constant region of the pool RNA. The unlabeled 22-nt RNA was present at 2.5 μM (squares) or 20 μM (triangles). **Fig. 7 (right).** Enhancement of ligation activity with successive rounds of selection. Pool autoligation activities were assayed as in Fig. 4A (pools 0 to 4) or as in (*33*) (pools 5 to 10) with the ligation buffer and temperature cycling of the initial rounds of ligation (Fig. 3). The uncatalyzed ligation rate of the oligonucleotides that mimic the pool RNA reaction (Fig. 6) was also assayed with the buffer of the initial ligation rounds. The uncatalyzed ligation rate expected with temperature cycling was interpolated from ligation rates from separate 12-day incubations at 25° and 37°C.

5 through 7; at each cycle random mutation created new genetic diversity, while selection for ligation promoted the survival and propagation of the fittest variants. The activity of the pool of ribozymes continued to improve during these three rounds of selection. An additional three cycles (rounds 8 to 10) were then performed without mutagenic amplification so that rare improved variants that arose during the earlier mutagenesis would increase in abundance so that they could be detected. During these last three cycles, the stringency of the ligation incubation was gradually increased by decreasing the Mg^{2+} concentration because the pool activities had increased to the point that decreasing the duration of the ligation incubation was no longer technically feasible. The improvement in ligation activity (almost 300-fold) resulting from six rounds of directed in vitro evolution is readily apparent by comparing the time courses of the pool 4 and pool 10 RNA ligation reactions (Fig. 4, A and B).

Both the catalyzed and the uncatalyzed reactions depend on the presence of a divalent cation (Fig. 6), as do all known ribozyme reactions. The Mg^{2+} optimum of the pool 10 ribozymes was lower than the Mg^{2+} optimum of the pool 7 ribozymes, presumably in response to the selection pressure for function at lower Mg^{2+} concentrations after round 7. Although the activity improvement between rounds 7 to 10 was greatest at lower Mg^{2+} concentrations, the pool 10 RNA was more active at all Mg^{2+} concentrations tested, even at a concentration nearly 100 times higher than that used during the ligation incubations of the final rounds of selection. The Mg^{2+} dependence of the uncatalyzed reaction was assayed by incubating the substrate oligonucleotide with a 22-nucleotide (nt) RNA identical to the pool 5′ constant region (Fig. 6). The plot of uncatalyzed rate against Mg^{2+} concentration is consistent with a single saturable Mg^{2+}-binding site ($[Mg^{2+}]_{1/2}$ = 119 ± 8 mM, V_{max} = 5.0 (± 0.2) × 10^{-6} per hour, values ± standard error). At low Mg^{2+} concentrations, ligation of pools 10 and 7 was more strongly dependent on the concentration of Mg^{2+} than the uncatalyzed oligonucleotide ligation (Fig. 6). The slope of these plots suggests that at least three Mg^{2+} ions must bind before catalysis. The rate acceleration of the pool 10 RNA over the uncatalyzed reaction was greatest at 15 mM Mg^{2+}, where the catalyzed rate was 7 million times faster than the uncatalyzed rate (3.8 per hour compared to 5.4 × 10^{-7} per hour) (Fig. 6).

Since the uncatalyzed reaction was template-dependent, enhanced binding of the ligating RNAs to the template might have accounted for a significant portion of the 7 millionfold rate acceleration. However, when the 22-nt RNA analogous to the 5′ constant region of the pool RNA was replaced with an RNA designed to form a very stable stem loop at its 5′ terminus (*13*), the rate of the uncatalyzed oligonucleotide ligation increased only 40 percent. Since these two uncatalyzed reactions proceed with similar rates, stabilization of the interaction between the 5′-terminal nucleotides of the pool and the template can contribute little to the rate acceleration afforded by the selected sequences; at least 5 millionfold must come from other mechanisms. Similarly, increasing the concentration of the 5′ constant region oligonucleotide did not lead to faster uncatalyzed ligation (Fig. 6), indicating that the substrate concentrations used in the catalyzed reactions are far above the K_d (dissociation constant) of the substrate-template complex.

The initial rate of the ligation reaction was determined for each enriched pool under the high Mg^{2+} conditions of the initial rounds of selection (Table 1 and Fig. 7). The pool activity rose above the background, uncatalyzed rate after the second round of selection, and the activity of the RNA pool increased with each round of selection thereafter. Comparison of pool 10 and uncatalyzed ligation rates under these high-Mg^{2+} incubation conditions revealed that the ligation rate of pool 10 RNA (8 per hour, $t_{1/2}$ = 5 minutes) was 3 million times faster than the uncatalyzed ligation rate (2.4 × 10^{-6} per hour, $t_{1/2}$ = 33 years). This uncatalyzed rate is in close agreement with the 3 × 10^{-6} per hour rate observed with pool 0 RNA.

Population changes during directed evolution. Restriction analysis revealed that each round of selection had a significant effect on the number of sequences remaining in the selected ribozyme pool and on the relative abundances of these sequences (Fig. 8). Since each independent sequence contains restriction sites at different random locations, the different individuals in a population yield different fragments after restriction digestion; the population structure can therefore be displayed on a sequencing gel. Pool DNA was ^{32}P-labeled at one end and cut with a combination of Alu I, Mse I, and Taq I endonucleases to cleave more than 90 percent of the pool molecules at least once within their 220 bp of random sequence. In the early rounds (pools 0 to 2), no sequences were enriched to the point that their corresponding bands could be detected above the background. However,

by round 3, more than 65 different enriched sequences were visible. Although each band in the round 3 and 4 lanes represents a homogeneous enriched sequence (except for a few coincident bands and rare spontaneous mutations), each band from later rounds represents a family of related sequences that was created by PCR mutagenesis of a single ancestral sequence. A sequence family that yields a 60-nt fragment dominated the pool by round 7, but by round 10 was largely supplanted by a family that yields a 76-nt fragment.

The selected sequence families displayed many evolutionary scenarios (Fig. 8). Most of the sequences that thrived in early cycles appear to be extinct by round 10, presumably because they could not compete in the harsh environment of increasingly stringent ligation conditions. Others maintained a relatively constant abundance. The ancestral sequences of a number of round 10 sequence families were not visible in round 4; these families are likely to be progeny of formerly inefficient catalysts that subsequently acquired advantageous mutations.

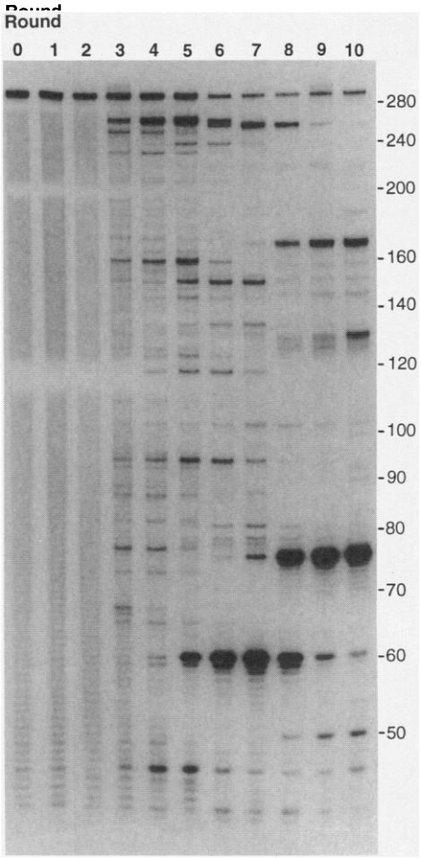

Fig. 8. Relative abundances of sequences in the selected ribozyme pools. Double-stranded DNA from each of the indicated rounds was ^{32}P-labeled at one end, then digested with a combination of Alu I, Mse I, and Taq I endonucleases, which recognize ACGT, TTAA, and TCGA, respectively (*36*). Restriction fragments were separated on a 5 percent acrylamide–7 M urea gel. The positions of marker DNA fragments (from a DNA sequencing ladder) with the specified number of nucleotides (50 through 280) are indicated.

The structure of the final selected population was also investigated by cloning and sequencing pool 10 DNA. A single family of sequences dominated this pool. Most members of this family have an Mse I site at position 76 and correspond to the band at position 76 in Fig. 8. However, some have point mutations at this site and give rise to the band at position 168 (due to an Mse I site at position 168). Bands at these two positions contain 70 percent of the radioactivity in the pool 10 lane, in good agreement with the representation of this family among the sequenced clones (11 out of 15 sequences). The 11 sequenced members of this family differ from the consensus by an average of 13 mutations. Of the several clones assayed, clone 4 (Fig. 9) is the most active, with an initial ligation rate slightly faster than that of pool 10.

Efficiency of selected ribozymes. The ribozymes that we isolated from the initial random sequence pool, without mutagenesis and optimization, were only moderately active catalysts, with rate accelerations of 10^3 to 10^4. Nevertheless, these rate accelerations compare favorably to those of typical catalytic antibodies, which are isolated after a stage of in vivo evolutionary optimization (maturation) of binding to an analog of the transition state of the reaction, with subsequent screening for the subsets that are catalytic (*14*). We suggest that there is an advantage to selecting directly for catalysis, as opposed to the indirect procedures used to isolate catalytic antibodies. In addition, many more RNA sequences can be initially sampled than is possible during the primary immune response (*15*); however this numerical advantage may be offset by the use of an established structural framework in all antibodies.

A modest degree of in vitro evolution led to a several hundredfold improvement in the catalytic efficiency of the pool of selected ribozymes. The observation that many sequence families could only be detected after mutagenesis and further selection is consistent with our original assumption that most of the catalytically active sequences present in the original pool would be suboptimal representatives of a given class of ribozymes. Our best "evolved" ribozymes enhance the rate of RNA ligation, making it 7 million times faster than that of the uncatalyzed template-directed reaction; this enhancement is comparable to that of the best existing catalytic antibodies (*16*). It will be of interest to see the extent to which ribozymes and catalytic antibodies can ultimately be optimized, and to see whether ribozymes selected in vitro can catalyze the impressive range of reactions catalyzed by antibody enzymes (*14*).

A rate acceleration of 7 million is much less than that achieved by most modern protein enzymes. The rate of RNA elongation by T7 RNA polymerase, one of the most efficient polymerases, is 230 nucleotides per second (*17*). This represents a rate 3×10^{11} times faster than our measured uncatalyzed reaction rate (*18*), and is 10^5 times faster than the average pool 10 ribozyme. The *Tetrahymena* group I ribozyme has been estimated to catalyze cleavage at the 5′ splice site 10^{11} times faster than the uncatalyzed reaction (*19*), suggesting that RNA enzymes may also be capable of polymerase-like rate accelerations of 10^{11}. It is not clear how much more improvement could be attained by further cycles of directed evolution of pool 10 RNA. Some improvement appears possible since pool 10 contains minor sequences (represented, for example, by 90- and 98-nt fragments in Fig. 8) that increase dramatically in abundance during the last round of selection.

A group II self-splicing intron catalyzes condensation between a template-bound oligonucleotide 2′- or 3′-hydroxyl and the 5′-triphosphate of the leader sequence of the intron, with the release of pyrophosphate (*20*). Whether any of our selected catalysts bear structural similarities with group II introns remains to be seen.

Implications for the RNA world hypothesis. The new ribozymes that we have isolated from a pool of random sequences

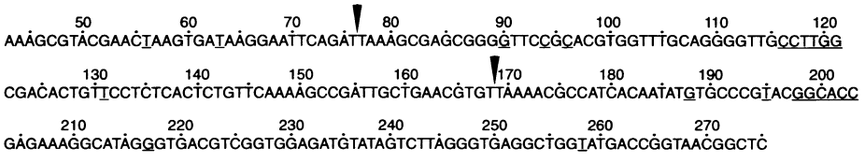

Fig. 9. Sequence of one of the isolated ribozymes. Members of pool 10 DNA were cloned (TA Cloning, Invitrogen) and sequenced. The sequence of the central 233 nucleotides of clone 4 is shown. Sequences of the 5′ constant region (bases 1 to 42) and the 3′ constant region (bases 276 to 295) are described in (*29*). Sty I and Ban I restriction sites used in pool construction are underlined. The 10 bases that differ from the consensus sequence of the dominant pool 10 sequence family are also underlined. Consensus bases at these positions are 56A, 63A, 90A, 94T, 96T, 131C, 188A, 195A, 217A, and 258A.

catalyze a chemical transformation similar to that catalyzed by polymerases. Their abundance in the random-sequence pool is therefore relevant to the hypothesis that life began with an RNA replicase that originated from prebiotically synthesized random-sequence RNA. We detected about 65 sequences (Fig. 8, pools 3 and 4) capable of carrying out a particular ligation reaction in a pool of more than 10^{15} initial sequences, or a frequency of occurrence of one in about 2×10^{13} sequences. This number is an underestimate of the abundance of the less active ribozymes, since many of these would have failed to ligate during the first round. A few of the selected sequences in pool 4 (one in about 3×10^{14} initial sequences) must be more active than the average activity of pool 4 RNA (0.03 per hour, or a rate acceleration of about 10^4). Presumably, sequences capable of acting as efficient template-directed RNA polymerases are more rare than this, and sequences capable of acting as an RNA replicase are even more rare. Evidently, catalysts of moderate activity could arise spontaneously from relatively small quantities of RNA (and perhaps related polynucleotides); however, a catalyst with the activity, accuracy, and dual functionality (enzyme and template) of an RNA replicase would be so rare that it could only arise spontaneously and in a single step from a truly enormous amount of RNA. The problem is compounded because two such sequences would be required for autocatalytic replication to begin, one to act as the polymerase and a second to act as the template. Therefore, an RNA replicase could only have arisen from primordial sequence pools that were not truly random. Joyce and Orgel anticipate this difficulty and propose that nonenzymatic, template-copying reactions may have had a dual role in generating primordial sequence pools that are more likely to give rise to a replicase (*21*). The initial pool may have been biased in favor of local secondary structure by a mechanism involving intermittent use of intramolecular sequence as the template. In addition, some sort of nonenzymatic catalysis was probably necessary for the initial copying of the replicase sequence to generate a molecule that could be used as a template, the copying of which by the replicase would generate more replicase molecules, thus initiating the autocatalytic explosion of life.

In the course of attempting to measure the uncatalyzed rate of our RNA ligation, we have detected a new type of template-dependent oligonucleotide condensation reaction. In previous studies of uncatalyzed RNA condensation reactions, imidazole, methylimidazole, or other activating groups were used (*22*) rather than pyrophosphate to activate the 5′ α-phosphate. Although the condensation of pyrophosphate-activated oligonucleotides is very slow, nucleoside 5′-polyphosphates are thought to be more plausible prebiotic molecules than nucleoside 5′-phosphorimidazolides (*23*). Furthermore, we have found that the pyrophosphate-activated oligonucleotide reaction appears to have a very high preference for the formation of 3′,5′- rather than 2′,5′-phosphodiester bonds. The previously studied condensation reactions display a wide range of regiospecificities, from preferentially 2′,5′ to preferentially 3′,5′. The choice of metal ions (*24*), activating group (*25*), and sequence of the ligation junction (*26*) have a marked influence on the degree of regiospecificity. The degree to which the observed regiospecificity of the pyrophosphate-activated reaction is dependent on these factors or on the extensive hybridization of the substrates to the template remains to be determined.

We initially assumed that our selection would favor ribozymes that yield a 3′,5′-linkage, since the ligated RNAs must be copied by reverse transcriptase into a full-length cDNA in order to be selectively amplified. We were surprised that reverse transcriptase only paused and did not terminate at a 2′ linkage in the template (*27*). Therefore, the catalyzed reaction does not appear to have been subjected to selection for regiospecificity, and the observed specificity may simply reflect acceleration of the uncatalyzed reaction with no change in mechanism.

The ribozymes that we have selected provide a new starting point for the evolution or design of RNAs with RNA polymerase and replicase activity. A series of issues including sequence-independent primer-template binding, the use of mononucleotide triphosphates as substrates, fidelity, and product-template dissociation now need to be addressed before an RNA replicase activity, an activity that has probably been extinct for over 3 billion years, can be fully resuscitated.

REFERENCES AND NOTES

1. For a review, see G. F. Joyce, *Nature* **338**, 217 (1989).
2. M. D. Been and T. R. Cech, *Science* **239**, 1412 (1988); J. A. Doudna and J. W. Szostak, *Nature* **339**, 519 (1989); J. A. Doudna, S. Couture, J. W. Szostak, *Science* **251**, 1605 (1991).
3. R. Green and J. W. Szostak, *Science* **258**, 1910 (1992).
4. For a review, see J. W. Szostak, *Trends Biochem. Sci.* **17**, 3 (1992).
5. For instance, the probability of finding a contiguous 20-nt element in a sequence with 220 random bases is about 18 times greater than that of finding the element in a sequence with 30 random positions, whereas a specific 8-bp stem is about 308 times more likely to be found in the longer sequence, if we assume that the loop joining the two arms of the stem can be any sequence and any length greater than 3 nucleotides. The combinatorial advantage of increased random region length is more striking when calculating the probability of finding more complex RNA structures.
6. R. Green, A. D. Ellington, D. P. Bartel, J. W. Szostak, *Methods Compan. Methods Enzymol.* **2**, 75 (1991).
7. Cloned ribozymes do not precipitate under the same conditions, presumably because these RNAs form more stable intramolecular contacts, and the remaining single-stranded regions are much less likely to find complementary segments on other molecules because only a single sequence is present. Both DNA pools and RNA pools with as few as 72 random positions also aggregate when incubated with 50 mM $MgCl_2$ (J. R. Lorsch, C. Wilson, J. W. Szostak, unpublished observations).
8. Even when the autoligation activities of individual cloned sequences were assayed, the reaction was not linear with respect to time. A similar phenomenon seen in group I intron self-splicing reactions has been attributed to misfolding of a subset of the ribozyme molecules [F. Michel *et al.*, *Genes Dev.* **6**, 1373 (1992)].
9. A fraction of the 16-hour pool 0 reaction of Fig. 4A was enriched for ligated molecules on an oligonucleotide affinity column as described for the pool 4 selected RNA, allowing detection of the small fraction of ligated molecules when resolved on a denaturing gel as in Fig. 4A. The ligation rate was calculated from the fraction of RNA retained on the column (0.000066), the typical column efficiency (0.65), and the fraction of enriched RNA that was ligated (0.47).
10. A. A. Beaudry and G. F. Joyce, *Science* **257**, 635 (1992); N. Lehman and G. F. Joyce, *Nature* **361**, 182 (1993).
11. T. Pan and O. C. Uhlenbeck, *Biochemistry* **31**, 3887 (1992); *Nature* **358**, 560 (1992).
12. R. C. Cadwell and G. F. Joyce, *PCR Methods Appl.* **2**, 28 (1992), found that addition of Mn^{2+}, and increasing concentrations of Mg^{2+}, enzyme, and the pyrimidine deoxynucleotides leads to a mutation rate during PCR of about 0.66 percent in 10 doublings (done in 30 PCR cycles), with very little bias in the types of mutations generated. We modified this protocol to preserve more sequence complexity and to achieve higher mutation rates. After three cycles of error-prone PCR (100-μl reaction, 50 ng of template DNA, 4-minute extension time), 50 ng of product (slightly more than one-eighth of the reaction) was removed, brought up to 100 μl with reaction buffer, and subjected to another three cycles of error-prone PCR. This procedure was repeated until the desired number of DNA doublings had been achieved. Gel purification was usually required after about 60 doublings. Our modification of the procedure of Cadwell and Joyce leads to a strong bias in the types of mutations generated. Comparative analysis of 11 sequences of the dominant pool 10 sequence family (Fig. 9) indicates that, of the 140 point mutations, three of the transversion possibilities were underrepresented (57 A·T to T·A, 46 A·T to G·C, 3 A·T to C·G, 0 C·G to G·C, 26 C·G to T·A, 8 C·G to A·T).
13. This RNA (pppGGAUAGAGCAAUCUAUCCGACUGGCACC) differs from the 5′ constant region of the pool RNA in that the 5′-most nucleotides are designed to form a 7-bp stem with a stable "tetra loop" [C. R. Woese, S. Winker, R. R. Gutell, *Proc. Natl. Acad. Sci. U.S.A.* **87**, 8467 (1990)] rather than a 3-bp stem with a 6-nt loop.
14. R. A. Lerner, S. J. Benkovic, P. G. Schultz, *Science* **252**, 659 (1991).
15. T. Honjo and S. Habu, *Annu. Rev. Biochem.* **54**, 803 (1985); S. Tonegawa, *Nature* **302**, 575 (1983).
16. Two catalytic antibodies provide rate enhancements of about 6 and 3 million, respectively [A. Tramontano, A. A. Ammann, R. A. Lerner, *J. Am. Chem. Soc.* **110**, 2282 (1988); K. D. Janda, M. I. Weinhouse, D. M. Schloeder, R. A. Lerner, S. J. Benkovic, *ibid.* **112**, 1275 (1990)]. Although catalytic antibodies are not covalently linked to their substrates, the rate enhancement of our catalysts and catalytic antibodies can be compared because they both represent saturated enzyme. Rate accelerations of some other very efficient catalytic antibodies [P. Wirsching, J. A. Ashley,

S. J. Benkovic, K. D. Janda, R. A. Lerner, *Science* **252**, 680 (1991)] cannot be compared with those of our catalysts because these antibodies catalyze second-order reactions. Our uncatalyzed reaction is pseudo–first order because we assay the ligation of stable substrate-template complexes.
17. M. Golomb and M. Chamberlin, *J. Biol. Chem.* **249**, 2858 (1974).
18. The T7 RNA polymerase elongation rate was determined in 20 mM $MgCl_2$ at 37°C (*17*). Uncatalyzed oligonucleotide ligation proceeds at 7×10^{-7} per hour in 20 mM $MgCl_2$ at 25°C (Fig. 7) and generally four times faster at 37°C than at 25°C.
19. D. Herschlag and T. R. Cech, *Biochemistry* **29**, 10159 (1990).
20. M. Morl, I. Niemer, C. Schmelzer, *Cell* **70**, 803 (1992).
21. G. F. Joyce and L. E. Orgel, in *The RNA World*, R. Gestland and J. Atkins, Eds. (Cold Spring Harbor Press, Cold Spring Harbor, NY, 1993), chap. 1.
22. L. E. Orgel, *J. Theor. Biol.* **123**, 127 (1986).
23. R. Lohrmann, *J. Mol. Evol.* **6**, 237 (1975).
24. P. K. Bridson and L. E. Orgel, *J. Mol. Biol.* **144**, 567 (1980).
25. T. Inoue and L. E. Orgel, *ibid.* **162**, 201 (1982).
26. J. Ninio and L. E. Orgel, *J. Mol. Evol.* **12**, 91 (1978).
27. D. P. Bartel and J. W. Szostak, in preparation.
28. The 110-nt N72 DNA, 5′-AACACTATCCGACT*GGCACC*-N72-*CCTTGG*TCATTAGGATCC (Ban I and Sty I sites are italicized), was synthesized and gel-purified (yield, 150 μg). A 3:3:2:2 molar ratio of A, C, G, and T phosphoramidites was used to synthesize the 72 random positions to compensate for the faster coupling rates of G and T phosphoramidites. Primer extension experiments indicated that up to 79 percent of the gel-purified product had chemical lesions that block second-strand synthesis. Therefore, this synthesis yielded 31.5 μg of DNA that could be amplified by PCR (5.2×10^{14} different sequences). The 110-nt N76 DNA, 5′-CGGGACTCTGA*CCTTGG*-N76-*GGCACC*TGTCCACGCTC, was synthesized, purified, and analyzed in the same manner and contained 96 μg of amplifiable DNA (1.6×10^{15} different sequences). The N72 and N76 pools were amplified in large (200 ml) PCR reactions for six and four cycles, respectively. After phenol extraction and precipitation, N72 DNA was cut with either Sty I (500 μg of DNA, 20,000 units of enzyme, 40-ml reaction) or Ban I (500 μg, 6000 units of enzyme, 20-ml reaction). N76 DNA was digested with both Sty I and Ban I. The N72–Sty I, N72–Ban I, and N76–Bam I–Sty I fragments were purified on a nondenaturing acrylamide gel. Ligation of the three fragments (3.5 nmol of each fragment, T4 DNA ligase, 1.1-ml reaction) was efficient and yielded predominantly the desired full-length three-piece product (80 percent yield). Pool 0 DNA was cloned and partial sequences of 11 randomly chosen clones indicated that the nucleotide distribution within the random-sequence segments fell within acceptable limits (A:C:G:T = 380:418:429:330 = 25:26:27:21).
29. The sequence of pool 0 DNA is 5-TTC*TAATAC-GACTCACTATA*GGAACACTATCCGACTGGCAC-C-N_{72}-CCTTGG-N_{76}-GGCACC-N_{72}-CCTTGGT-CATTAGGATCCCG (T7 promotor is italicized). The pool 0 RNA begins with the G immediately flanking the T7 promotor. Pool 0 DNA was amplified with 42- and 20-nt primers corresponding to the 5′ and 3′ constant regions, respectively.
30. Pool RNA and a twofold molar excess of biotinylated DNA (5′-biotin-CGGGATCCTAATGAC-CAAGG) were denatured in water (80°C, 3 minutes) and allowed to cool briefly at room temperature before the addition of streptavidin-agarose (SA) binding buffer (30 mM tris, pH 7.4, 500 mM NaCl, 1 mM EDTA, 0.25 percent NP-40, 0.1 percent SDS). After 5 minutes at room temperature, a suspension of SA beads (Sigma) in binding buffer was added; the mixture was rocked for 20 minutes, and then poured into a column for washing and buffer equilibration. In round 1, a total of 160 ml of SA suspension containing 18 ml of SA was added to a 40-ml annealing reaction mixture that contained 4 mg of pool 0 RNA. In later rounds, much less RNA and smaller volumes were used; by round 4, a 2-ml SA suspension was added to 0.25 ml of annealed pool.
31. Synthetic DNA-RNA chimeric substrate oligonucleotides that contain a DNA tag sequence [$(dA)_{22}$, $(dT)_{22}$, or 5′-dAA*GCATCTAAGCATCT-C*AAGCAAA] followed by the RNA sequence 5′-CCAGUC were used with their cognate oligonucleotide affinity columns [oligo(dT)-cellulose type 7 (Pharmacia), oligo(dA)-cellulose type 7 (Pharmacia), $(dT)_{25}$ magnetic beads, or d*GAGATGCT-TAGATGCA*-Teflon (Glen Research)], as indicated in Table 1 (italics indicate segments of complementarity).
32. The selective PCR primers had the following DNA sequences $(A)_{22}$-CCAGTC, $(T)_{22}$-CCAGTC, and AAGCATCTAAGCATCTCAAGCA. Other primers were the same as those used in the pool 0 amplification (*29*).
33. Although the pool RNA of rounds 6 to 10 was not immobilized on the agarose before the ligation reaction, the RNA was subjected to an annealing treatment that approximated the temperatures and salt conditions of the immobilization and preliminary incubation procedures of initial rounds: RNA and an excess of biotinylated oligonucleotide were denatured in water (3 minutes, 80°C) and allowed to cool for a brief period at room temperature before the addition of the non-magnesium components of the ligation buffer. After 10 minutes, $MgCl_2$ was added and the reaction was incubated another 10 minutes. The reaction was started by addition of substrate oligonucleotide and stopped with EDTA (100 mM). Prior to selection on the oligonucleotide affinity column, the stopped ligation mixture was passed through streptavidin-agarose beads to retain the pool RNA and wash off unreacted substrate. The pool RNA was then eluted from the column and selected as in Fig. 3. When the ligation reaction contained RNA from later rounds and was analyzed directly without enrichment for ligated molecules (for example, in the time courses of Figs. 4B, 5B, 6, and 7), the pool RNA was not typically annealed to the biotinylated oligonucleotide but instead was annealed to a non-biotinylated oligonucleotide of the same sequence.
34. Phosphate compounds were detected with ammonium molybdate and reduced vanadyl chloride [R. M. C. Dawson, D. C. Elliott, W. H. Elliott, K. M. Jones, *Data for Biochemical Research* (Clarendon Press, Oxford, ed. 3, 1986), p. 486].
35. G. Volckaert and W. Fiers, *Anal. Biochem.* **83**, 228 (1977).
36. Pool DNA was amplified by PCR with the use of the biotinylated primer (*30*) that hybridizes to the 3′ constant region of the pool DNA. After purification on an agarose gel, the PCR product was end-labeled. The biotin moiety at the 3′ constant region of the pool RNA blocked labeling so that the DNA was labeled only on the end of the 5′ constant region. Restriction digestions were performed in the presence of plasmid carrier DNA; monitoring the extent of the carrier DNA digestion confirmed that the digestions were complete.
37. We thank R. Green for helpful discussions and J. R. Lorsch, K. B. Chapman, R. W. Roberts, and other members of the laboratory for careful reading of this manuscript. Supported by grants from Hoechst AG and NASA.

5 May 1993; accepted 25 June 1993

Physical Chemistry of the $H_2SO_4/HNO_3/H_2O$ System: Implications for Polar Stratospheric Clouds

M. J. Molina, R. Zhang, P. J. Wooldridge, J. R. McMahon, J. E. Kim, H. Y. Chang, K. D. Beyer

Polar stratospheric clouds (PSCs) play a key role in stratospheric ozone depletion. Surface-catalyzed reactions on PSC particles generate chlorine compounds that photolyze readily to yield chlorine radicals, which in turn destroy ozone very efficiently. The most prevalent PSCs form at temperatures several degrees above the ice frost point and are believed to consist of HNO_3 hydrates; however, their formation mechanism is unclear. Results of laboratory experiments are presented which indicate that the background stratospheric H_2SO_4/H_2O aerosols provide an essential link in this mechanism: These liquid aerosols absorb significant amounts of HNO_3 vapor, leading most likely to the crystallization of nitric acid trihydrate (NAT). The frozen particles then grow to form PSCs by condensation of additional amounts of HNO_3 and H_2O vapor. Furthermore, reaction probability measurements reveal that the chlorine radical precursors are formed readily at polar stratospheric temperatures not just on NAT and ice crystals, but also on liquid H_2SO_4 solutions and on solid H_2SO_4 hydrates. These results imply that the chlorine activation efficiency of the aerosol particles increases rapidly as the temperature approaches the ice frost point regardless of the phase or composition of the particles.

Polar stratospheric clouds (PSCs) play a crucial role in the depletion of ozone (O_3) in the polar stratosphere in the winter and spring months: They promote the conversion of stable inorganic chlorine compounds ($ClONO_2$ and HCl) into a photolytically active form (Cl_2), enabling the formation of the chlorine radicals Cl and ClO that participate in catalytic O_3 destruction processes (*1, 2*). Furthermore, the PSC particles facil-